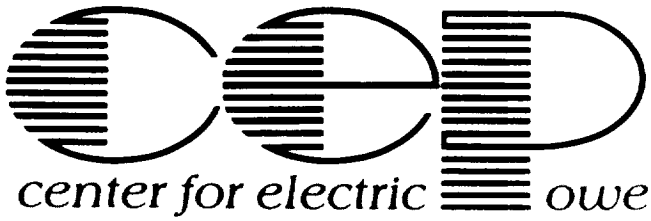

Investigation of the Collision Line Broadening Problem as Applicable to the NASA Optical Plume Anomaly Detection (OPAD) System: Phase I

Report D-V-95-1
Final Report
Grant NAG8-206

Submitted by:

Timothy C. Dean
Carl A. Ventrice
Center for Electric Power
Department of Electrical Engineering
Tennessee Technological Univeristy
Cookeville, TN 38505

Submitted to:

National Aeronautics and Space Administration
George C. Marshall Space Flight Center
Marshall Space Flight Center, AL 35812

May 31, 1995

Tennessee Technological University
P.O. Box 5032
Cookeville, Tennessee 38505

Investigation of the Collision Line Broadening Problem as Applicable to the NASA Optical Plume Anomaly Detection (OPAD) System: Phase I

Since the Fall semester of 1991, the Tennessee Tech Center for Electric Power and the Department of Electrical Engineering have been working in conjunction with NASA Marshall Space Flight Center (MSFC) on solving the collision line broadening problem as it applies to the OPAD project. Dr. C.A. Ventrice has been the faculty advisor/researcher for this project along with Paige Youngkins who was with the project from Fall 1991 to Fall 1992 and Tim Dean who has been with the project from Spring 1993 to present. Funding for this project, NASA grant NAG8-206, began with the NASA Fiscal Year 1992 and ended at the end of NASA Fiscal Year 1994. Although no funding is being received from NASA at this point, the research is continuing in this area in order to both better understand the problem and to maintain a relationship with the NASA MSFC.

As a final report for phase I of the project, the researchers are submitting to the Tennessee Tech Office of Research the following two papers: "Collision Line Broadening Effects on Spectrometric Data from the Optical Plume Anomaly System (OPAD)," presented at the 30th AIAA/ASME/SAE/ASEE Joint Propulsion Conference, June 27-29, 1994 in Indianapolis, and "Calculation of Collision Cross Sections for Atomic Line Broadening in the Plume of the Space Shuttle Main Engine (SSME)," presented at the IEEE Southeastcon '95, March 26-29, 1995, in Raleigh. These papers fully state the problem and the progress made up to the end of NASA Fiscal Year 1994.

Phase II of the project will consist of further research into the mechanisms of collision line broadening in order to more accurately model the phenomenon. Verification of the current collision broadening model along with any subsequent models will involve comparison with data obtained at the Diagnostic Test Facility, Stenis Space Center. The researchers at Tennessee Tech intend to share the results of this research with NASA in order to further the OPAD project.

AIAA 94-2984
Collision Line Broadening Effects on Spectrometric Data from the Optical Plume Anomaly Detection System (OPAD)

T.C. Dean and C.A. Ventrice
Tennessee Tech University
Cookeville, Tennessee
T.L. Wallace
Vanderbilt University/NASA/Svt-AEDC
Tullahoma, Tennessee
W.T. Powers and A.E. Cooper
NASA/MSFC
Marshall Space Flight Center, Alabama

30th AIAA/ASME/SAE/ASEE Joint Propulsion Conference
June 27-29, 1994 / Indianapolis, IN

COLLISION LINE BROADENING EFFECTS ON SPECTROMETRIC DATA FROM THE OPTICAL PLUME ANOMALY DETECTION SYSTEM (OPAD)

T.C. Dean and C.A. Ventrice
Tennessee Technological University
Cookeville, Tennessee

T.L. Wallace
Vanderbilt University/NASA/Svt-AEDC
Tullahoma, Tennessee

W.T. Powers and A.E. Cooper
NASA/MSFC
Marshall Space Flight Center, Alabama

Abstract

The NASA OPAD system has been devised to predict concentrations of anomalous species in the plume of the Space Shuttle Main Engine (SSME) through analysis of spectrometric data. Self absorption of the radiation emitted by these anomalous species can strongly influence this data. The self absorption of radiation is highly dependent on the line shape of the atomic transition of interest. This paper discusses the methods used to predict line shapes of atomic transitions in the environment of a rocket plume. The Voigt profile is used as the line shape factor since both Doppler and collisional line broadening are significant. The collisional line widths are given by an expression obtained from classical kinetic theory that is dependent on the collisional cross sections of the atomic species with the perturbing species. Methods used to determine the collisional cross sections are discussed and the results are given and compared with experimental data. These collisional cross sections are then incorporated into the current self absorbing radiative model and the predicted spectrum is compared to actual spectral data collected from the Stennis Space Center (SSC) Diagnostic Test Facility (DTF) rocket engine.

I. Introduction

The use of plume emission spectrometry for the health monitoring of liquid fueled rocket engines is a technology which, although still in development, has proven to provide useful data about rocket engine tests.[1] However, the development of this technology has required new research into modeling the physics of a liquid fueled rocket engine plume and new developments and innovations in processing and interpreting spectral data from the rocket plumes. During the past two years, improvements in instrumentation, spectral data pre-processing, plume codes, spectral modeling, computer technology, and spectral analysis have been incorporated into the OPAD operations. These enhancements have improved functionality and increased objectivity for spectral analysis and result in improved engine diagnostic capability. An overall second generation of capabilities, both in terms of instrumentation and data analysis has been achieved through application of new technologies.

Multiple organizations and laboratories have been enlisted to provide the required skills. A diversified OPAD team has formed around the original efforts of Marshall Space Flight Center Astrionics Laboratory and Sverdrup at Arnold Engineering Development Center (AEDC) to propel the initial concept and insights to fruition. Members of this team included personnel at NASA/Ames Research Center, The University of Alabama, Vanderbilt University, and Tennessee Technological University. In addition, Stennis Space Center as a part of the OPAD group has supplied MSFC with important spectral data from the DTF and A1 test stands. This paper will give a brief discussion of the evolution of the OPAD program to present. Additionally, this paper will focus on the research being conducted at Tennessee Technological University in the area of collision line broadening effects as applicable to the OPAD program.

II. The Evolution of OPAD

Background

The process of applying spectroscopy to the SSME for plume diagnostics, as it exists today, originated at MSFC in Huntsville, Alabama, and its implementation was assured largely through the efforts of Sverdrup Technologies site operations personnel at the Air Force AEDC in Tennessee. This process, OPAD, has formed the basis for various efforts in the development of in-flight plume spectroscopy and in addition produced a viable test stand vehicle health monitor. OPAD is currently implemented on stands at MSFC and the Stennis Space Center in Mississippi.

The process of reviewing engine failures occurring during SSME development testing revealed,[2] in the films of the firings, indications of various anomalous occurrences. It was proposed that if a plainly visible event occurred, perhaps the onset of that event would yield luminosity below the visible threshold which could serve as a precursor to a major failure. To investigate that possibility, a project[3] was enacted to analyze and characterize the emitted spectra from rocket plumes. The purpose was to identify spectra peculiar to verified mechanical anomalies, and then devise a system capable of detecting those spectra and yielding appropriate outputs in response to them..

The basic method used for investigation is that of spectral emissions, primarily from the shock structure in the plume referred to as the "mach disc." Because of the high temperatures in the disc, most metals radiate with sufficient intensity to allow detection of only a few parts-per-million or less. The chosen method works well for atmospheric stands but is not useful for either altitude (diffuser) stands or for actual flight vehicles, since altitude stands have no mach

disc and launched vehicles lose the disc at altitude. The emission method does allow the acquisition of full spectra, thus permitting the study of more than just species emission. To cover the "no mach disc" condition, as well as providing a relatively simple system light weight enough to fly, an absorption system might be a choice.

Spectral measurements and spectral models have been in use since the late 1960's[4] at AEDC to determine the constituents of engine exhaust plumes. Most of these measurements are performed to determine flow-field properties and species concentrations of molecular reactants, using techniques such as emission, resonance absorption, electron beam impact excitation, and most recently Laser Induced Fluorescence (LIF) to determine free-atomic species concentrations. While many excellent validated line-by-line (LBL) radiative transfer codes have been developed and are available for molecular species, essentially no comprehensive validated models were available for analysis of atomic spectral data.

To meet this need, AEDC and MSFC initiated an effort in 1990[5] to develop LBL radiative transfer models to provide quantitative analysis of spectral data from the OPAD health monitoring program currently being applied to the SSME. The present model, *SpectraV*, is the result of experience gained over the past four years with predicting the spectra of atomic species. Developed with the goal of an in-flight system in mind, *SpectraV* provides not only the basis for quantitative plume spectral analysis for the present SSME instrumentation configuration, but has been developed to be applicable to future emission/absorption/LIF configurations which may be used near the nozzle exit plane of the SSME of other propulsion systems. After model validation is complete, *SpectraV* will, in combination with data processing algorithms, provide quantitative

estimates for species erosion rates (grams/sec) and associated uncertainties and allow for real-time usage at the test stand or control facilities.

Instrumentation

The program was started using the capabilities of AEDC[3] and was first operated at the only atmospheric test stand then conveniently available, A1 at SSC. Some data were taken at the A3 stand at Santa Suzanna Test Facility also. As soon as the MSFC test bed was ready, operations were moved there, leaving a presence at SSC to continue acquiring data. Examination of the data made it quite obvious that the then available commercial instrumentation would not be economically feasible for this task and, thus, the design of custom instrumentation was undertaken. Initially, that instrumentation consisted of two devices--the Reticon Array Spectrometer (RAS), also referred to as the SuperOMA, and the Polychromator; the former is a 4096 channel linear array spectrometer and the latter is a 16 channel spectroradiometer. The former delivers the complete spectrum, but is relatively slow, and the latter yields high operational speed at the expense of spectral content. Occasional extra data were taken using a commercial OMA. Those instruments served well from 1988 until the present. More recently a newly designed triple spectrometer has been put in place with the hope of acquiring data faster and with less noise than has been the norm. The new device has three sections, each of which is a complete spectrometer but which operates together from one set of input optics, thus allowing much flexibility in the ways one might configure the output. Having cooled detectors, it is also capable of better sensitivity through the reduction of background noise. The OPAD Polychromator has undergone a significant hardware and spectral configuration upgrade which

improves both versatility in terms of transition line selectivity, and near ideal background subtraction capability for selected transitions.

Other hardware improvements during the past year include the acquisition of a Silicon Graphics workstation with a gigabyte storage capacity. It provides the robust computational platform for development of AI techniques.

III. Effect of Spectral Line Broadening on Determination of Species Concentrations

Types of Broadening

There are three principle ways in which a transition line is broadened: natural, Doppler, and collisional broadening. Natural line broadening is most always insignificant when either Doppler or collisional line broadening is present; therefore, its effects will be neglected in the broadening calculations. Doppler broadening occurs due to the thermal motion of the species which are emitting the radiation. The normalized lineshape which results is

$$L_D(\nu) = \frac{1}{b_D}\sqrt{\frac{\ln 2}{\pi}}\exp\left(-\frac{(\nu-\nu_0)^2 \ln 2}{b_D^2}\right), \tag{1}$$

where ν_0 is the line center frequency and b_D, the Doppler halfwidth at half maximum (HWHM), is defined as

$$b_D = \nu_0\sqrt{\frac{2kT\ln 2}{mc^2}} \tag{2}$$

where k is Boltzmann's constant, T is the temperature of the gas, m is the mass of the emitting species, and c is the speed of light in a vacuum. Since for a given species this lineshape is a function of temperature only, it is not difficult to incorporate into a radiative model. Collisional line broadening results from the presence of other atoms and molecules, perturbers, in the gas

mixture with the emitting species. These perturbers "collide" with the excited species causing a random dephasing of the emitted radiation. Collisional line broadening, often called Lorentz broadening, yields

$$L_L(\nu) = \frac{b_c/\pi}{(\nu-\nu_0)^2 + b_c^2} \tag{3}$$

as the normalized lineshape. This lineshape is called the Lorentz lineshape. Determining the value of b_c, the collisional HWHM, is often quite difficult and will be discussed in a later section.

In situations, such as the plume of the SSME, where Doppler and collisional broadening are both significant, the Voigt lineshape must be used. The Voigt lineshape,

$$L_\nu(\nu) = \frac{a\sqrt{\ln 2}}{\pi^{3/2} b_d} \int_{-\infty}^{\infty} \frac{\exp(-x^2)}{a^2 + (x-y)^2} dx \tag{4}$$

$$a = \frac{b_c\sqrt{\ln 2}}{b_d}, \qquad y = \frac{\sqrt{\ln 2}}{b_D}(\nu - \nu_0), \tag{5),(6}$$

is the convolution of the Doppler and the Lorentz lineshapes. The *a* parameter is called the damping constant. The integral cannot be evaluated in closed form; thus, numerical methods are required to solve the integral. This will be the lineshape used in the radiative model for the OPAD program. Figure 1 shows a comparison of the different lineshapes where the Lorentz and Doppler lineshape have the same HWHM and the Voigt lineshape is the convolution of the two.

Self Absorption

Self absorption occurs when the radiation emitted from an atom (molecule, ion, etc.) does

not leave the excited medium (e.g. flame, rocket engine plume) but is absorbed by another atom of the same type. In the absence of self absorption, optically thin case, the amount of energy emitted from the plume due to radiation of a given species is directly proportional to the concentration of that species in the plume. However, when some of this radiation is reabsorbed the dependence becomes non-linear. Figure 2 shows the effect of self absorption on the lineshape of a sodium transition at a concentration of 1 part per billion (ppb) in an environment similar to the DTF. Figure 3 shows the effect of self absorption on the emitted intensity of the radiation by plotting the emitted intensity as a function of the concentration of sodium. This intensity is what will be measured by a spectrometer viewing the plume. Figure 4 is a graph of the fraction of the emitted energy that is reabsorbed as a function of the sodium concentration. Refer to Wallace *et al*[1] or Dean and Ventrice[6] for further discussion of self absorption effects on lineshape and emitted intensity.

IV. Collision Modeling

Classical Broadening Theory

Classically an excited atom is considered to emit a continuous sinusiodal wave. According to Mitchell and Zemansky[7], if each collision that the atom experiences causes a random dephasing of the wave then the expression for the half-width (HWHM) is $b_C=Z_C/\pi$ where Z_C is the number of broadening collisions per second per emitting atom. From classical kinetic theory[7], assuming ideal gas behavior, the value of b_C can be determined as

$$b_c = \sum_{i=1}^{n} P_i \sigma_i^2 \sqrt{\frac{2}{\pi^3 k T}\left(\frac{1}{m_i}+\frac{1}{m_e}\right)}, \qquad (7)$$

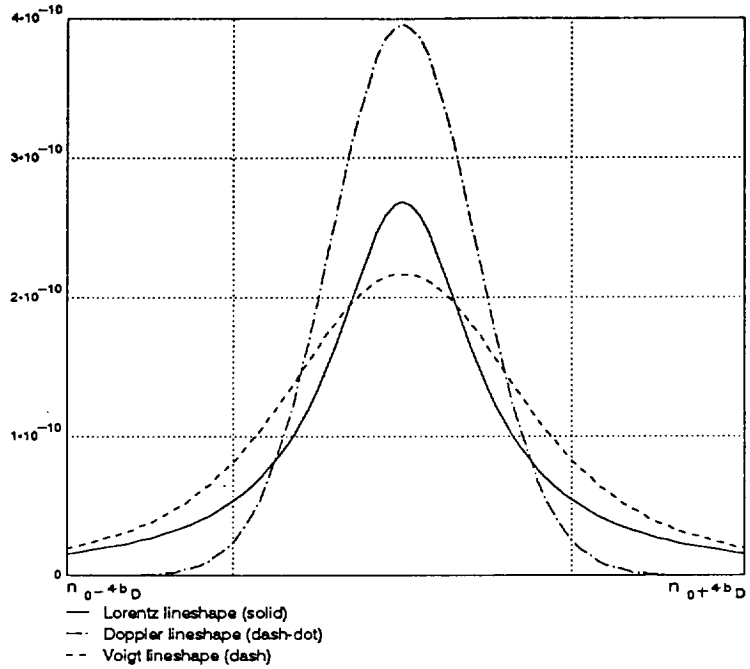

Fig. 1. Comparison of lineshapes

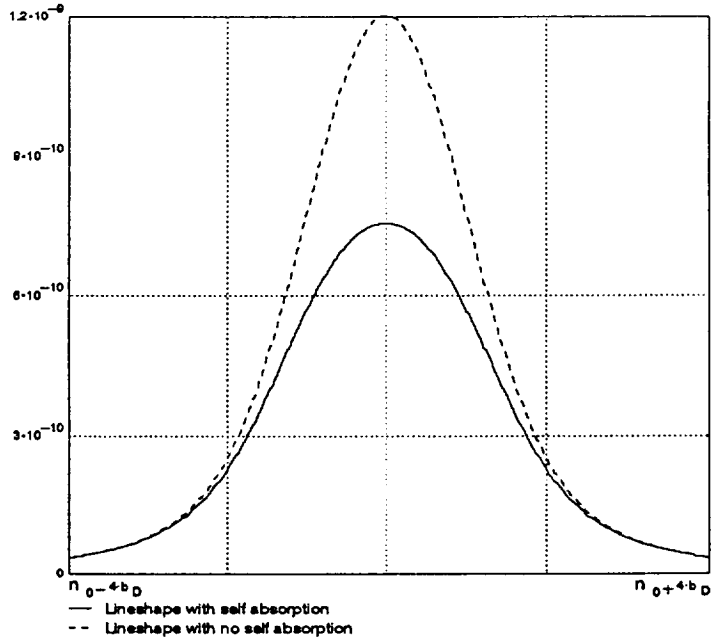

Fig. 2. Self absorption effect on lineshape

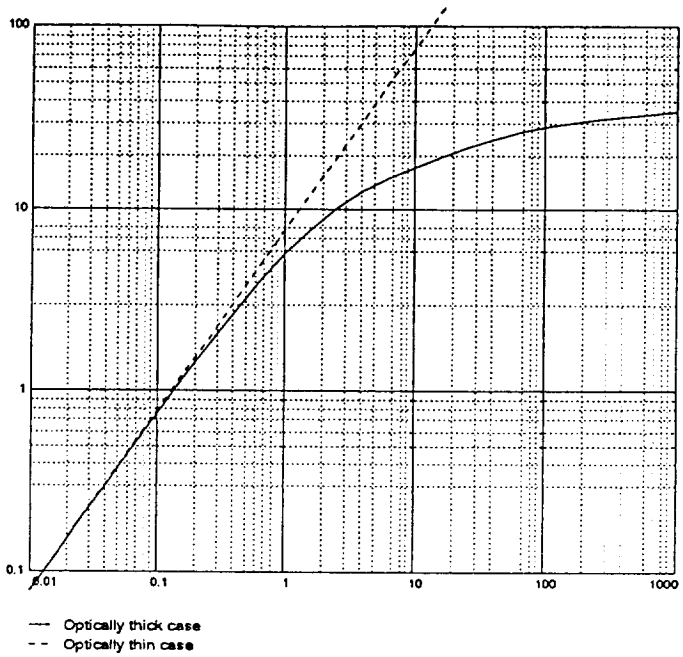

Fig. 3. Intensity (watts/m^2-str) of radiation emitted from medium versus species concentration (ppb)

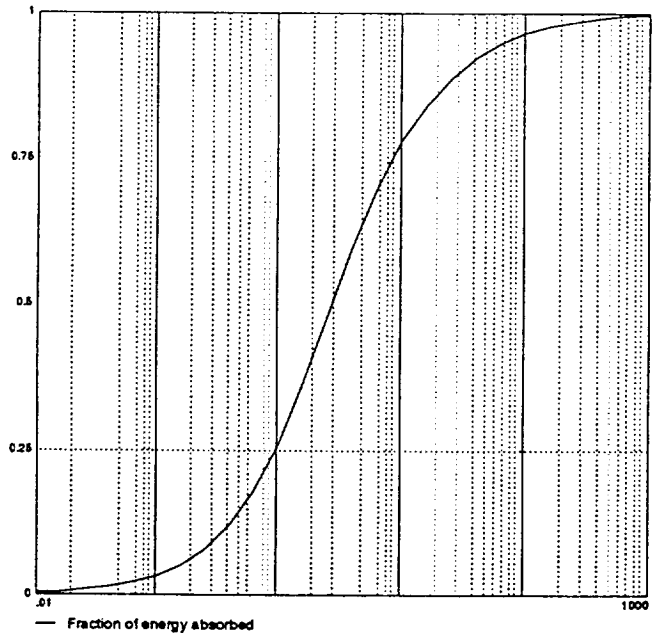

Fig. 4. Fraction of energy absorbed versus species concentration (ppb)

where n is the number of perturbers, P_i is the partial pressure of the i*th* perturber, σ_i^2 is the broadening collision cross section of the emitter with the i*th* perturber, m_i is the mass of the i*th* perturber, m_e is the mass of the emitter, k is Boltzmann's constant, and T is the temperature. Combustion modeling techniques can be used to determine all of the parameters of equation (7) except for the broadening collision cross section.

Broadening Collision Cross Section

The broadening collision cross sections of the emitter with the perturbers are difficult to determine exactly. Therefore, as a first order approximation the molecules and atoms are assumed to be rigid spheres and all collisions are assumed to be broadening collisions. This leads to the collision cross section being determined as

$$\sigma_i^2 = \pi (r_i + r_e)^2, \tag{8}$$

where r_i and r_e are the rigid sphere radii of the i*th* perturber and the emitter respectively, see figure 5. This brings up the task of determining the rigid sphere radius of all emitting species of interest and of all perturbing molecules. Values for atomic radii can be found in chemistry reference manual; however, these values are based on density measurement of the solid state of the atoms and may not be applicable for the high temperature gaseous environment of a rocket engine plume; therefore, another method must be used to determine these values. Also, rigid sphere radii for the H_2O and H_2 molecules can be found in Hirschfelder *et al.*[8], but it should be noted that these radii are distances at which significant intermolecular interactions occur. However, the interactions that cause collision line broadening result in only slight perturbations

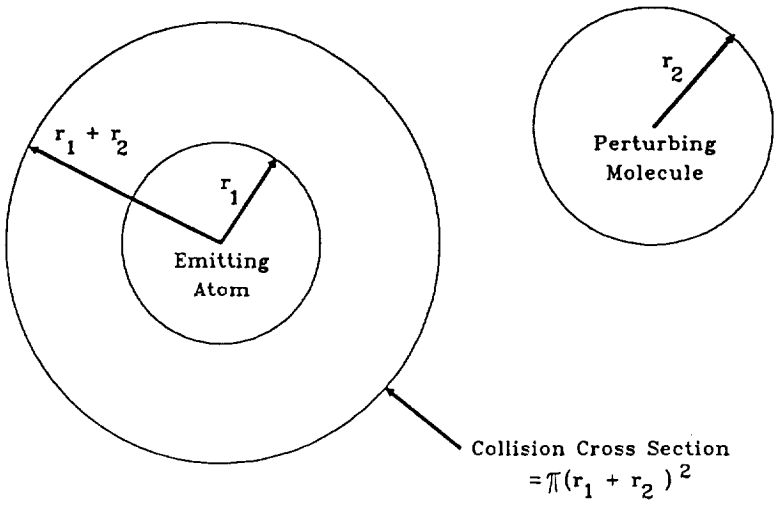

Fig. 5. Rigid Sphere Collision

(on the order of 1 part per million) of the energy of the emitting atom and should probably not be categorized as significant.

Determining Rigid Sphere Radii

As can be inferred from the previous section, the rigid sphere radii that are being pursued here are not the same as those used in gas kinetic relationships, but rather could be termed the radius of broadening interaction. Determination of these radii involve the interpretation of experimental data. Most experimental research in the determination of broadening parameters of specific elements in specific flames define an effective molecular weight of the perturbers in the flame and thus determine an effective collision broadening cross section for the element with all of the perturbers. This technique results in the determined cross section being dependent on the specific mole fractions of perturbers present in the flame.

The data obtained by McGee and Winefordner[9] give broadening parameters for several elements in H_2-O_2 and C_2H_2(acetylene)-O_2 flames. Two different gas mixture ratios, standard

and fuel-rich, were used for each flame. These different mixtures provided two different mole fraction ratios for each flame which can be used to better determine the effect of the individual perturbers on each element. Based on the assumption that the primary perturbers in the hydrogen-oxygen flames are H_2O and H_2, Table I gives the collision cross section of each element with H_2O and H_2. With the exception of Rb and Na, all elements have a greater collision cross section with H_2O than with H_2, and Magnesium and Zinc seem to have unusually large $\sigma_{H_2O}^2/\sigma_{H_2}^2$ ratios. The larger $\sigma_{H_2O}^2$'s could possibly be explained by the H_2O molecule being

Table I. Collision Cross Sections

Element	$\sigma_{H_2O}^2$	$\sigma_{H_2}^2$
Cu	590	190
Li	172	140
Mg	411	37.7
K	212	109
Rb	58.3	95.7
Ag	199	156
Na	146	251
Zn	279	10.3

Note: For comparison with reference 9, divide values listed here by π.

a polar molecule and thus having a longer range interaction than the non-polar H_2 molecule. With the given data, determining actual radii to associate with each atom or perturbing molecule is not possible in a rigorous sense, but for the purposes of comparison with experimental data the collision cross sections listed here will be adequate. However, for future study, an attempt will be made to correlate the experimental data with the published atomic radii and the

commonly used intermolecular potential functions (Lennard-Jones, Buckingham, etc.[8]) to see if the definition of a radius of broadening interaction for individual species is feasible.

Effect of Temperature on Molecular Rigid Sphere Radius

At the elevated temperature of the mach disc of the SSME (approximately 2700K) some molecules will be in excited, vibrational or rotational, states possibly causing the nominal rigid sphere radius to be increased. The effects of the vibrational excitation of the hydrogen molecule on the rigid sphere radius of the molecule were investigated using the quantum mechanical anharmonic oscillator approximation. A computer program was written to determine the wavefunctions of the anharmonic oscillator at the different allowed energy levels of the hydrogen molecule. Given the wavefunction, Ψ_n, for the n*th* vibrational level, the average deviation from the nominal internuclear separation of the hydrogen atoms can be calculated by

$$\overline{\Delta x_n} = \int_{-\infty}^{\infty} \Psi_n^*(x)\, x\, \Psi_n(x)\, dx, \tag{9}$$

where Ψ_n^* denotes the complex conjugate of Ψ_n. The calculated probability density functions associated with the wavefunctions, $P_n(x)=\Psi_n^*(x)\Psi_n(x)$, for the ground state and the first two excited states of the H_2 molecule are shown in figure 6. By assuming a Maxwell-Boltzmann population distribution at a given temperature, the percentage of molecules in each state of excitation can be determined. This distribution is given by

$$F_n(T) = \frac{\exp(-\frac{\mathscr{E}_n}{kT})}{\sum_i \exp(\frac{-\mathscr{E}_i}{kT})}, \tag{10}$$

where F_n is the percentage of molecules in the n*th* state, $\mathscr{E}_n$ is the energy of the n*th* excited

vibrational state, k is Boltzmann's constant, and T is the temperature. The effective rigid sphere radius can be calculated by using

$$R(T) = R_0 + \frac{1}{2}\sum_n \overline{\Delta x_n} F_n(T), \tag{11}$$

where R_0 is the nominal rigid sphere radius. The change in the rigid sphere diameter of the hydrogen molecule at the temperature of the mach disc, about 2700K, was 0.424 percent; therefore, for the present level of approximation the expansion of the rigid sphere radius was considered negligible. The effect of vibrational excitement on the rigid sphere radius of thewater molecule was also assumed to be negligible.

Kang and Kunc[10] have devised a method for determining molecular radii in high temperature gases using a different technique that includes the effects of rotational excitation in addition to the vibrational excitation. The rigid sphere radius of an excited molecule given a specific vibrational and rotational state is

$$R_{\nu,J} \approx R_0 + \frac{9}{4}\beta l_\alpha^2 \exp[2(\beta l_\alpha)^{1/2}(\nu - 1)] + \frac{2l_\alpha^4}{R_e^3}J^2, \tag{12}$$

where β and l_α are parameters describing the oscillation of the molecule, ν and J are the vibrational and rotational quantum numbers respectively, and R_e is the equilibrium internuclear separation. The values used for the quantum numbers are the gas mean vibrational quantum number and the most probable rotational quantum number. If these parameters are computed

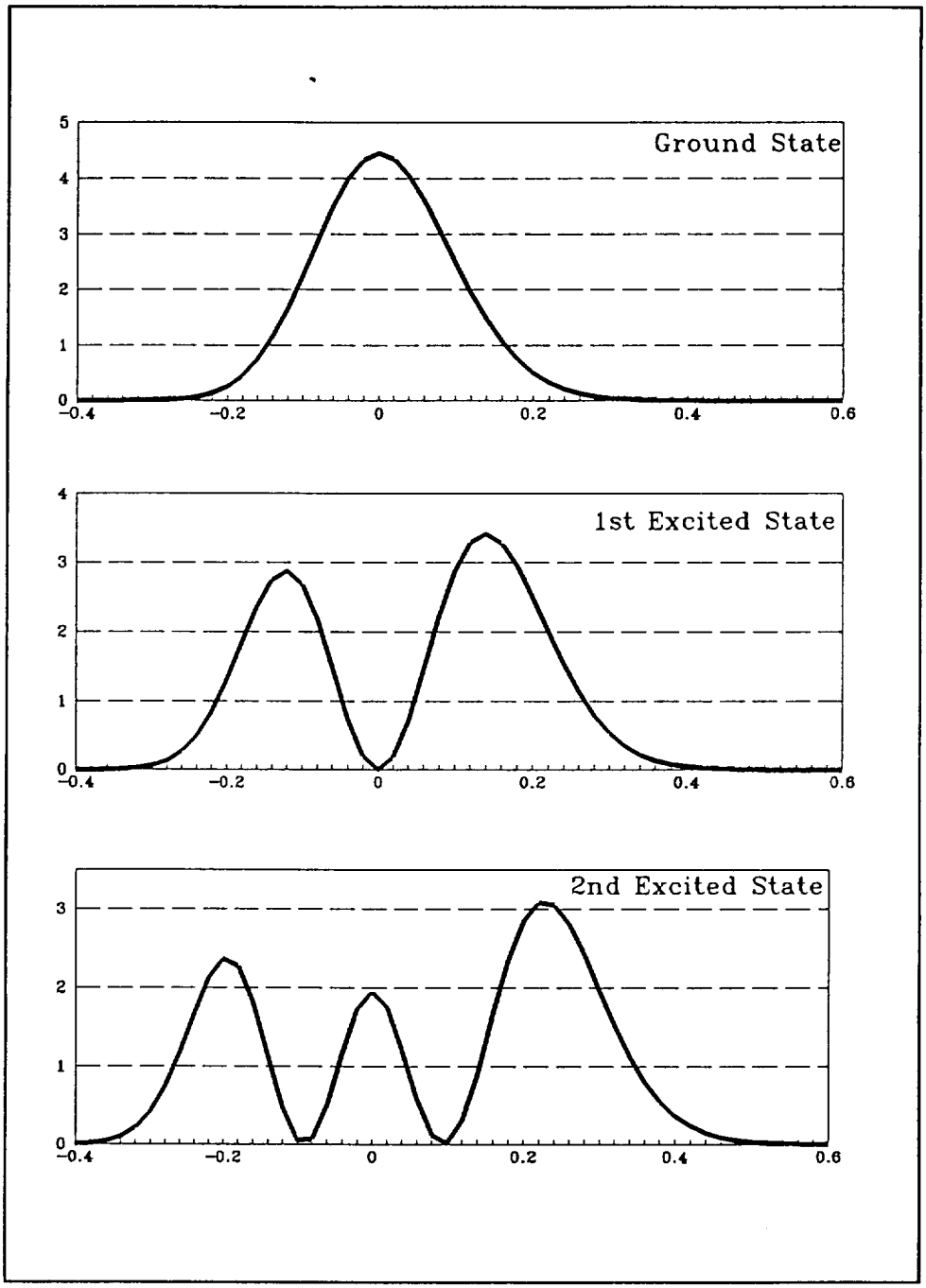

Figure 6-This figure shows the probability density functions associated with the ground, first, and second excited state of the H_2 molecule. The x-axis is in angstroms and the zero point is referenced to the equilibrium internuclear separation.

for the hydrogen molecule at 2700K, the expansion of the rigid sphere radius is 1.51 percent. If this increase is included in the calculations of the line widths due to collision broadening, the change in the line widths is less than 0.8 percent.

V. Comparison of Experimental and Theoretical Results

The DTF at SSC has conducted tests by seeding the plume of a rocket engine with known concentrations of a species in order to determine the emitted intensity that would result. The data for nickel and chromium will be used here for comparison purposes since these are elements of concern to the OPAD program and the atomic transition data is available. Although Table I contains no information on collision cross sections for the chromium and nickel atoms, the published atomic radii for the elements are quite close to that for copper (copper - 1.28Å and chromium and nickel- 1.25Å[11]) and the same collision cross sections will be assumed for the sake of comparison.

Table II shows the data used in the radiative model to determine the calculated emitted intensities versus concentration. These intensities are frequency integrated and represent intensities that would be recorded by a wideband spectrometer such as the OPAD spectrometer. Figures 7 and 8 show the comparison of the DTF and calculated data for nickel and chromium, respectively. As can be seen there is a significant discrepancy between the DTF data and the calculated intensities. In order to determine the cause of the discrepancies an error analysis was performed using the radiative model for chromium. The intensity versus concentration curves were broken into two regions, optically thin and optically thick, with the boundary being the point where 10 percent of the emitted radiation is absorbed. Four parameters (temperature, pressure, path length, and collision cross section) were chosen and varied by ± 10 percent. The

average change in each region of the curve along with the change in the transition point from optically thin to optically thick were then computed. The results follow in Table III. From these results, temperature is obviously the most significant parameter in the radiative model which means that accurate determination of the temperature of the mach disc region of the plume is imperative. One factor not considered in the error analysis is the fraction of the element seeded into the plume that actually appears in the mach disc region of the plume as a free atom and not an ion or molecule. This factor would simply cause the DTF data curve to shift to the left, thus causing better agreement with the predicted values.

VI. Conclusions

With the goal of determining species concentrations in the plume of the SSME via analysis of spectral data, the necessity of modeling the effects of collisional line broadening on the line shape of emitted radiation has been shown. However, due to a lack of experimental data

Table II. Radiative Model Parameters

Parameter	Nickel	Chromium
Wavelength (Å)	3524.5	4254.3
Transition Probability $\times 10^8$ (1/sec)	1.0	0.315
Degeneracy (upper, lower)	5,7	9,7
$\sigma_{H_2O}{}^2$ (Å^2)	590	590
$\sigma_{H_2}{}^2$ (Å^2)	190	190
Partial Pressure of H_2O	2.0 atm	
Partial Pressure of H_2	0.8 atm	
Temperature[1]	3300 K	
Path Length[1]	0.1 m	

regarding the collision cross section of metallic species with perturbers such as H_2O and H_2, the magnitude of the broadening is difficult to determine. This fact warrants the continued investigation of the theories, both classical and quantum mechanical, of collisional line broadening. Also shown was the sensitivity of the radiative model to variations in the parameters of the model and the necessity of accurate determination of the temperature of the plume environment. With continued investigation into the modeling of collision effects on emitted radiation and into radiative properties and characteristics of the rocket engine plumes along with the use of the DTF data for comparison purposes the goal of the OPAD program is realizable.

Acknowledgements

The authors would like to thank the members of the OPAD team at Vanderbilt University, NASA-MSFC, NASA-Ames, AEDC-Arnold Air Force Base, and The University of Alabama for the support and help provided and the team at Stennis Space Center for providing the DTF data. This research was supported by NASA grant NAG8-206.

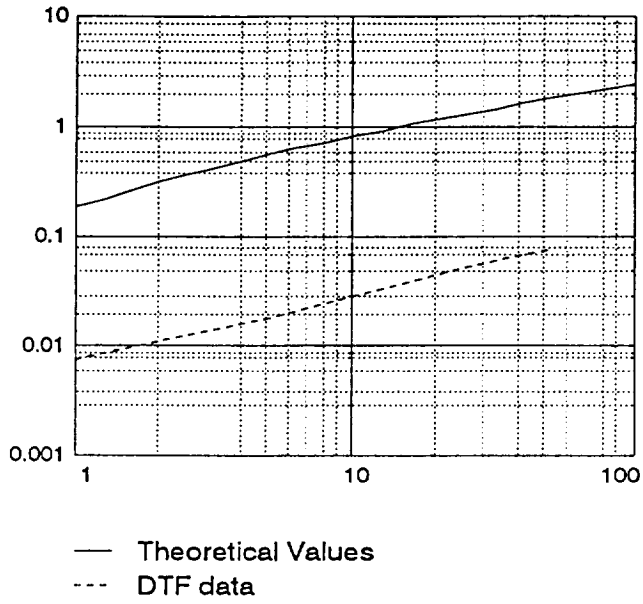

Fig. 7. Intensity (watt/m^2-str) of emitted radiation versus concentration (ppm) of nickel for the DTF data and calculated data.

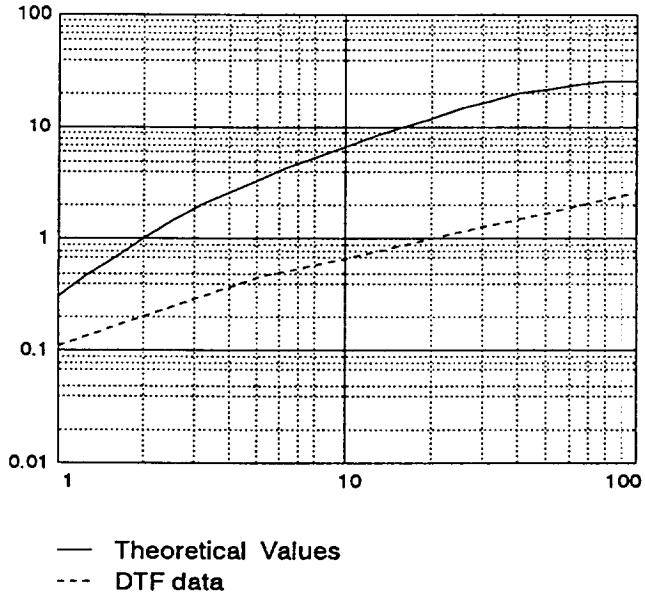

Fig. 8. Intensity (watt/m^2-str) of emitted radiation versus concentration (ppm) of chromium for the DTF data and calculated data.

Table III. Effects of Parameter Variation on Radiative Model				
Parameter	Amount of Variation (%)	Average Change from Normal (%)		Change in transition point (%)
		Optically Thin Region	Optically Thick Region	
Temperature	+10	131	268	5.79
	-10	-64.4	-127	-6.19
Collision Cross Section	+10	0.008	4.16	9.63
	-10	-0.007	-4.59	-9.83
Path Length	+10	10.0	11.3	-9.40
	-10	-10.0	-11.7	11.3
Pressure	+10	10.0	15.6	0.510
	-10	-10.0	-16.1	0.536

References

1. Wallace, T.L., Powers, W.T., and Cooper, A.E., "Simulation of UV Atomic Radiation for Application in Exhaust Plume Spectrometry", Paper presented at AIAA/SAE/ASME/ ASEE 29th Joint Propulsion Conference, June 28-30, 1993, Monterey, CA.

2. Cikanek, H.A. III: "Failure Characteristics of Space Shuttle Main Engine Failures," in proceeding of the Joint Propulsion Conference, June 1987.

3. Powers, W.T.; Cooper, A.E.; and Wallace, T.L.: "OPAD Status Report: Investigation of SSME Component Erosion," SAE Aerospace Atlantic Conference, Dayton, OH, April 1992.

4. McGregor, W.K.; Seiber, B.L.; and Few, J.D.: "Concentrations of OH and NO in YJ93-GE-3 Engine Exhausts Measured In Situ by Narrow-Line UV Absorption," AIAA No. 73-506, Denver, CO, 1973.

5. Wallace, T.L.; Cooper, A.E.; and Powers, W.T.: "Preliminary Analysis of SSME Baseline Plume Emissions," Second Annual Health Monitoring Conference for Space Propulsion Systems, Cincinnati, OH, November 1990.

6. Dean, T.C., and Ventrice, C.A., "Collisional Broadening of Atomic Species in SSME Plume Environment: Development of Radiative Model for Collisional Broadening Analysis", Unpublished Report, June 8, 1993.

7. Mitchell, A.C.G., and Zemansky, M.W.,"Resonance Radiation and Excited Atoms", Cambridge University Press, New York, NY, 1961.

8. Hirschfelder, J.O., Curtiss, C.F., and Bird, R.B., "Molecular Theory of Gasses and Liquids", John Wiley and Sons, Inc., New York, NY, 1967.

9. McGee, W.W., and Winefordner, J.D., "Measurement of the Damping Constant (the *a*-Parameter) of Several Elements in Several Hydrogen and Acetylene-Oxygen Flames using an Absorption Method", *J. Quant. Spectrosc. Radiat. Transfer,* **Volume 7**, pp. 261-272, 1967.

10. Kang, S.H. and Kunc, J.A., "Molecular Diameters in High-Temperature Gases," *Journal of Physical Chemistry*, Volume 95, No. 18, pp. 6971-6973, 1991.

11. Emsley, J., "The Elements", Oxford University Press, New York, NY, 1989.

Calculation of Collision Cross Sections for Atomic Line Broadening in the Plume of the Space Shuttle Main Engine (SSME)

T.C. Dean and C.A. Ventrice
Tennessee Technological University
Electrical Engineering Department
Cookeville, Tennessee 38505

IEEE Southeastcon '95

Raleigh, NC

March 26-29, 1995

CALCULATION OF COLLISION CROSS SECTIONS FOR ATOMIC LINE BROADENING IN THE PLUME OF THE SPACE SHUTTLE MAIN ENGINE (SSME)

T.C. Dean and C.A. Ventrice
Tennessee Technological University
Electrical Engineering Department
Cookeville, Tennessee 38505

Abstract - **An analytical method for determining the cross sections for collision line broadening by molecular perturbers is investigated using effective central force interaction potentials as proposed by Kunc. The Lennard-Jones potential is used throughout to describe the interatomic interactions. These cross sections are determined for several atomic species with H_2, one of the principal constituents of the SSME plume environment, and compared with experimental data. Agreement with experimental data within the range of experimental error is obtained for most atomic species.**

INTRODUCTION

The Optical Plume Anomaly Detector (OPAD) program is concerned with the detection and quantification of anomalous elements in the plume of the Space Shuttle Main Engine (SSME) during ground level test firings. The anomalous elements present in the SSME plume are usually the result of the erosion of engine parts; therefore, this system provides a reliable health monitoring and diagnostics tool for the engine. This system is based on the analysis of broadband spectrometer data obtained from the mach disc region of the plume. The atoms of the anomalous elements present in the plume will become excited as they pass through the hot shock structure of the mach disc and emit radiation at their characteristic wavelengths. The intensity versus wavelength profile obtained by the broadband spectrometer can then be analyzed in order to determine which elements of interest are present in the SSME plume.

Determining mass flow rate or number densities of the elements in the flow is complicated by the nonlinear dependence of the intensity on the number densities of the elements [1,2]. Due to the self absorption of the radiation at higher species concentrations, the intensity of the radiation at the characteristic wavelength of the species of interest is not a linear function of the species concentration. This self absorption effect is strongly dependent on the line broadening that occurs for the atomic transition of interest. As an atomic transition line broadens the radiative energy is spread over a broader range of frequencies causing the intensity of the radiation at a given frequency to be effectively reduced. This reduced intensity results in less radiation being self-absorbed. Therefore in order to effectively predict the amount of self absorption taking place, one must determine the extent to which the line is broadened.

Two types of line broadening, Doppler and collisional, are significant in the SSME mach disc region [2]. Doppler is dependent primarily on the temperature of the region and can be easily considered. However, collisional broadening depends on the temperature and pressure of the region along with the mole fractions of the individual perturbing species and the interaction energies between the atomic emitters and the molecular perturbers. Characteristics regarding the plume environment -- temperature, pressure, mole fractions, etc. -- can be obtained via flame analysis codes. This paper discusses a method for determining the broadening parameters for the interaction of metallic atoms with molecular perturbers.

INTERATOMIC POTENTIAL

To determine the amount of line broadening that occurs, we must first investigate the interatomic interaction potential function. Several different empirical forms for interaction potentials exist, but a commonly used form for the interaction of two non-polar molecules or

atoms is the Lennard-Jones (12-6) potential [3],

$$V(r) = 4\epsilon\left[\left(\frac{\sigma}{r}\right)^{12} - \left(\frac{\sigma}{r}\right)^{6}\right]. \tag{1}$$

The σ parameter is the inter-nuclear distance of closest approach when the particles collide with zero initial relative kinetic energy [3]. The ϵ parameter is the maximum energy of attraction and occurs at a distance of $r=2^{1/6}\sigma$. The r^{-6} term represents the long range attractive forces that exist between molecules and accurately represents the induced-dipole--induced-dipole interaction. The r^{-12} term represents the short range repulsive forces of two molecules. Figure 1 shows the form of the potential function.

One method for determining the values of the two parameters, σ and ϵ, of the Lennard-Jones potential is by using properties of the solid crystalline state of the substance of concern [3,4].

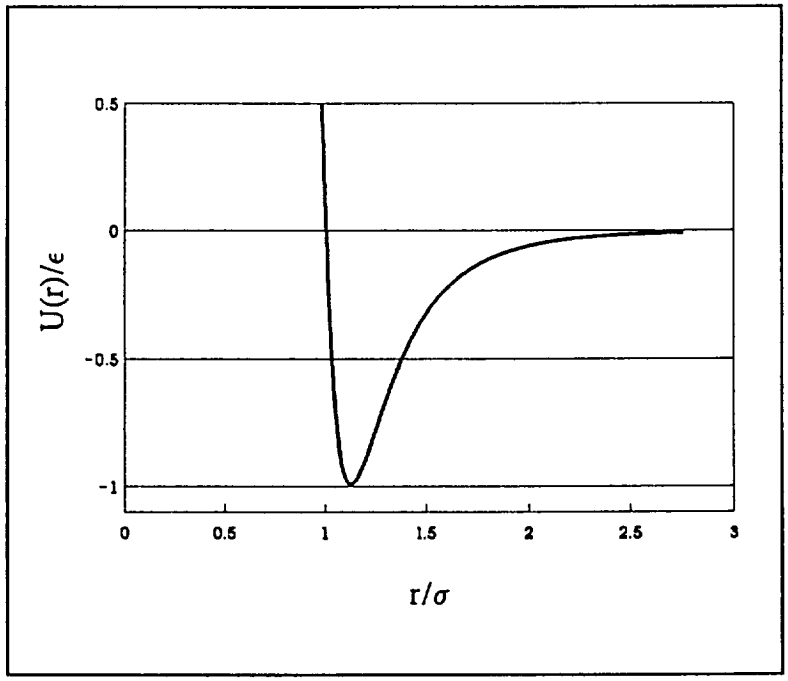

Figure 1. Lennard-Jones potential.

Assuming that the pair interaction potential of the crystal is given by (1) and that the forces between molecules (the term molecules will be used interchangeably with atoms) of the crystal are additive, the total potential energy of the crystal per mole is

$$\Phi = 2N_A\epsilon\left[\sum_{i=1}^{\infty}\left(\frac{\sigma}{r_i}\right)^{12} - \sum_{i=1}^{\infty}\left(\frac{\sigma}{r_i}\right)^{6}\right], \tag{2}$$

where N_A is Avogadro's number and r_i is the distance from a reference lattice site to the *i*th lattice site in the crystal. The factor of 2 in front of the equation comes from the factor of 4 in (1) and the fact that (2) involves the interaction of a pair of molecules. Since for a given crystalline structure the separation of a molecule from every other molecule is known, the summations in (2) can be evaluated and (2) can be written as

$$\Phi = 2N_A\epsilon\left[L_{12}\left(\frac{\sigma}{a}\right)^{12} - L_6\left(\frac{\sigma}{a}\right)^{6}\right], \tag{3}$$

where a is the characteristic nearest neighbor distance and L_n, the set of lattice sums, is defined as

$$L_n = a^n\sum_i r_i^{-n}. \tag{4}$$

These lattice sums have been tabulated for the different crystalline structures and are available from many sources [3,4]. When the crystal is in equilibrium, the nearest neighbor distance must be at the point where the potential energy is a minimum which can be located by differentiating (3) with respect to a which yields

$$\frac{\sigma}{a}=\left[\frac{L_6}{2L_{12}}\right]^{\frac{1}{6}}. \tag{5}$$

Substituting (5) into (3) and including the zero-point energy, Φ_0, gives

$$E=-\frac{N_A\epsilon}{2}\frac{L_6^2}{L_{12}}+\Phi_0 \tag{6}$$

the total energy of the crystal. The total energy of the crystal per mole is given by the enthalpy of sublimation of the substance at 0 K, $H_0^{(subl)}$. The zero-point energy of the crystal can be determined from the Debye temperature, θ_D,

$$\Phi_0=\frac{9}{8}N_A k\theta_D, \tag{7}$$

where k is Boltzmann's constant. Using equations (6) and (7) and $H_0^{(subl)}$, ϵ can be solved for as

$$\epsilon=\left(\frac{2H_0^{(subl)}}{N_A}-\frac{9}{4}k\theta_D\right)\frac{L_{12}}{L_6^2}. \tag{8}$$

Therefore the Lennard-Jones pair potential for almost any substance can be determined given the enthalpy of sublimation at 0 K, the Debye temperature, the crystalline structure, and the characteristic nearest neighbor distance of the crystal.

Determining the interaction potential of two unlike molecules can often be a difficult experimental task. Therefore, several combining rules have been developed that approximate

the interaction potential parameters for unlike molecules given the potential parameters for the like molecules. The Kong combining rule was developed for the Lennard-Jones potential [4] and is given by

$$\epsilon_{12}\sigma_{12}^{12}=\left(\frac{\epsilon_{11}\sigma_{11}^{12}}{2^{13}}\right)\left[1+\left(\frac{\epsilon_{22}\sigma_{22}^{12}}{\epsilon_{11}\sigma_{11}^{12}}\right)^{\frac{1}{13}}\right]^{13} \tag{9}$$

$$\epsilon_{12}\sigma_{12}^{6}=(\epsilon_{11}\sigma_{11}^{6}\epsilon_{22}\sigma_{22}^{6})^{\frac{1}{2}}, \tag{10}$$

where the subscripts on the parameters indicate which molecular interaction the parameter is referring to.

ATOM-MOLECULE CENTRAL FORCE POTENTIAL

In the plume of the SSME the primary perturbers of the atomic emitters are H_2O and H_2 molecules. Therefore, since we can determine the atom-atom interactions, we must use these potentials to determine an atom-molecule central force potential in order to calculate the broadening effects of the molecules on the atoms. Hot gas molecules tend to be excited either vibrationally or rotationally which causes the interaction potential with an atom to be dependent not only on the separation of the centers of mass but also on the angular orientation of the molecule. Using the method developed by Kunc [5] and outlined below, we shall determine an effective central force potential for a hydrogen molecule interacting with an atom.

In the Kunc approach, the atoms of the molecule are treated as individual atoms interacting with each other due to a Morse type potential and each atom of the molecule interacts with the

emitting atom according to some type of atom-atom interaction potential of arbitrary complexity, the Lennard-Jones potential for our case. Therefore, for a diatomic molecule interacting with an atom, three interaction potentials must be defined to cover the interaction of each atom with all other atoms. The atom-atom interaction can be represented in a general form by the following multipole expansion

$$V_{ij}(r_{ij}) = \sum_m \frac{C_{ij}^{(m)}}{r_{ij}^{n_m}}, \tag{11}$$

where the i and j subscripts refer to the individual atoms in the target and perturbing molecules, $C_{ij}^{(m)}$ is the coefficient of the mth term in the expansion, r_{ij} is the distance from the ith atom in the perturbing molecule to the jth atom in the target molecule, and n_m is the exponent associated with the mth term of the expansion. In the case of a molecule interacting with an atom, the j subscript will always be equal to 1; therefore, the second subscript will be dropped and the remaining subscript will indicate which atom of the perturbing molecule is being referred to. For the Lennard-Jones potential and the hydrogen molecule, $C_1^{(1)}=C_2^{(1)}=4\epsilon\sigma^{12}$, $C_1^{(2)}=C_2^{(2)}=-4\epsilon\sigma^6$, $n_1=12$, and $n_2=6$. Since the perturbing molecule may be oriented in any number of ways as it approaches the target atom the interaction potential of (11) must be averaged over all possible orientations yielding, after some mathematical manipulations,

$$\langle V^{(m)}(r)\rangle_i = \frac{C_i^{(m)}}{r^{n_m}} \sum_{p=0}^{\infty} \frac{A_{n_m}^{(p)} r_{m_i}^{2p}}{r^{2p}} \tag{12}$$

$$A_{n_m}^{(p)} = \frac{(n_m - 1)\, n_m\, (n_m + 1)\, (n_m + 2) \cdots (n_m + 2p - 2)}{(2p + 1)!}, \tag{13}$$

where r_{m_i} is the distance from the center of mass of the molecule to the nucleus of the ith atom in the molecule and r is the distance between the center of mass of the molecule and the nucleus of the target atom. According to Kunc, the infinite sum in (12) can be replaced by the sum of the first 25 terms with an uncertainty of less than one percent. The effective potential for the interaction of the molecule and the atom can then be given by

$$V(r) = \sum_i \sum_m \langle V^{(m)}(r) \rangle_i. \tag{14}$$

The value for r_{m_i} is dependent on the rotational and vibrational state of the molecule and has been calculated to be approximately 0.4Å for the hydrogen molecule at SSME mach disc temperatures ($\sim$3000K).

CROSS SECTION CALCULATION

General Theory

In developing the expression for the cross section for collision line broadening, we will proceed along the same lines as Hindmarsh and Farr [6]. Given a single electron oscillator, the displacement as a function of time can be written as

$$f(t) = \cos(\omega_0 t + \eta(t)), \tag{15}$$

where ω_0 is the unperturbed oscillator frequency and $\eta(t)$ is the departure in phase from the unperturbed oscillation due to collisions with the oscillating atom. The autocorrelation function

of the displacement function will be, neglecting small terms due to ω_o being in the optical frequency range and using Euler's equation,

$$\begin{aligned}\Phi(\tau) &= \frac{1}{2}[\cos(\omega_0\tau + \eta(t,\tau))]_t \\ &= \frac{1}{4}\{e^{i\omega_0\tau}[e^{i\eta(t,\tau)}]_t + e^{-i\omega_0\tau}[e^{-i\eta(t,\tau)}]_t\} \\ &= \Psi(\tau) + \Psi^*(\tau),\end{aligned} \tag{16}$$

where $\eta(t,\tau)=\eta(t+\tau)-\eta(t)$ and $[\,]_t$ indicates the expected value with respect to time. The Fourier transform of (16) will give the spectral intensity that results from the collisions with the oscillator:

$$I(\omega) = \int_{-\infty}^{\infty} \Psi(\tau)\, e^{i\omega\tau}\, d\tau + \int_{-\infty}^{\infty} \Psi^*(\tau)\, e^{i\omega\tau}\, d\tau. \tag{17}$$

The task now is to evaluate the expectation operation involved in the calculation of $\Psi(\tau)$.

The Impact Approximation

In order to evaluate the expectation operation and calculate $\Psi(\tau)$, it will be necessary to make the approximation that the duration of the collision is much smaller than the time between collisions. This is usually the case for gases at a temperature of a few hundred Kelvin, so for the mach disc temperature of approximately 3000K, the approximation should be quite accurate [6]. First consider the change in the quantity $\Psi(\tau)e^{-i\omega_0\tau}$ caused by a change $\Delta\tau$ in τ, where $\Delta\eta=\eta(t,\tau+\Delta\tau)-\eta(t,\tau)$:

$$\begin{aligned}\Delta[\Psi(\tau)e^{-i\omega_0\tau}] &= \frac{1}{2}[e^{i\eta(t,\tau)}(e^{i\Delta\eta}-1)]_t \\ &= \frac{1}{2}[e^{i\eta(t,\tau)}]_t[(e^{i\Delta\eta}-1)]_t \\ &= \Psi(\tau)e^{-i\omega_0\tau}[(e^{i\Delta\eta}-1)]_t .\end{aligned} \tag{18}$$

The second line of (18) is possible since $\Delta\eta$ is statistically independent of η. The number of collisions with an impact parameter of ρ which occur in the time interval $\Delta\tau$ is $N\bar{v}2\pi\rho\, d\rho\,|\Delta\tau|$ where N is the number density and $\bar{v}$ is the average relative velocity. The expectation operation can now be evaluated as

$$[e^{i\Delta\eta}-1]_t = 2\pi N\bar{v}|\Delta\tau|\int_0^\infty [e^{i\eta(\rho)}-1]\rho\, d\rho, \tag{19}$$

where $\eta(\rho)$ is the phase change that occurs due to a collision with impact parameter of ρ. Since the integral is in general a complex valued integral, we can define

$$\sigma_r = 2\pi\int_0^\infty [1-\cos\eta(\rho)]\,\rho\, d\rho \tag{20}$$

and

$$\sigma_i = 2\pi\int_0^\infty \sin\eta(\rho)\,\rho\, d\rho \tag{21}$$

such that

$$[e^{i\Delta\eta}-1]_t = -N\bar{v}|\Delta\tau|(\sigma_r - i\sigma_i). \tag{22}$$

We may then treat (18) as a differential equation since the average is over a large number of collisions. The differential equation is easily solved for $\Psi(\tau)$, and then using (17), neglecting small terms, and normalizing the following lineshape function can be derived:

$$I(\omega) = \frac{N\bar{v}\sigma_r/\pi}{(\omega_0 - \omega + N\bar{v}\sigma_i)^2 + (N\bar{v}\sigma_r)^2}. \tag{23}$$

From (23) it can be seen that σ_i is proportional to the shift of the line center and σ_r is proportional to the line width. This parameter σ_r is the cross section for broadening and is calculated by using (20) and the following expression for the phase shift for a given impact parameter collision

$$\eta(\rho) = \frac{2}{\bar{v}\hbar} \int_0^\infty \frac{V(R)R\,dR}{(R^2 - \rho^2)^{1/2}}, \tag{24}$$

where $\hbar$ is Planck's constant divided by 2π and $V(R)$ is the atom-molecule interaction potential.

RESULTS AND CONCLUSIONS

Using the above methods, the collision cross section for broadening by the hydrogen molecule was calculated for several different elements of interest to the OPAD program. The results are compared to data from flame tests of the elements in a H_2/O_2 burner which is a similar environment to the SSME engine [7]. The experimental data are collected for both a standard and a fuel rich flame and include broadening by H_2, H_2O, and other minor flame constituents.

The cross section for H_2 is extrapolated from the data assuming that broadening occurs only due to H_2 and H_2O. The calculated and experimental values are listed in Table 1. It should be noted that the experimental values given in Table 1 are subject to experimental errors possibly "somewhat larger" than 25 percent, [7], and thus the error propagating to the extrapolated values will be quite significant. This will account for a large portion of the discrepancy between the experimental and the calculated cross sections.

ACKNOWLEDGEMENTS

The authors would like to thank the members of the OPAD team for their help and support. This research was partially supported by NASA grant NAG8-206.

TABLE 1. Collision Cross Sections

Element	Cross Sections (Å^2)			
	Experimental [7]			Calculated from this work
	Standard	Fuel Rich	Extrapolated	
Ag	33.0	40.0	49.7	48.2
Cu	95.0	74.0	60.5	42.5
K	21.0	33.0	34.7	51.1
Li	29.0	30.0	44.6	41.6
Mg	60.0	37.0	12.0	43.7
Na	57.0	63.0	79.9	47.7
Zn	40.0	22.0	3.3	35.4

REFERENCES

[1] Wallace, T.L., Powers, W.T., and Cooper, A.E., "Simulation of UV Atomic Radiation for Application in Exhaust Plume Spectrometry", AIAA/SAE/ASME/ASEE 29th Joint Propulsion Conference, 1993, Monterey, CA.

[2] Dean, T.C., Ventrice, C.A., "Collision Modeling Techniques for Determining Line Broadening Effects in the Plume of the SSME," *Advanced Earth-to-Orbit Propulsion Technology-1994*, Vol. I, pp. 160-167.

[3] Hirschfelder, J.O., Curtiss, C.F., and Bird, R.B., Molecular Theory of Gases and Liquids, John Wiley and Sons, Inc., New York, NY, 1967.

[4] Maitland, G.C., Rigby, M., Smith, E.B., Wakeham, W.A., *Intermolecular Forces: Their Origin and Determination*, Clarendon Press, Oxford, 1981.

[5] Kunc, J.A., "Central-force potentials for interaction of rotationally and vibrationally excited molecules," *Journal of Physics B: Atomic, Molecular, and Optical Physics*,vol. 23, pp. 2553-2566.

[6] W. R. Hindmarsh, J. M. Farr, "Collision Broadening of Spectral Lines," *Progress in Quantum Electronics,* vol. 2, pp. 143-213, 1972.

[7] McGee, W.W., and Winefordner, J.D., "Measurement of the Damping Constant (the *a*-Parameter) of Several Elements in Several Hydrogen and Acetylene-Oxygen Flames using an Absorption Method", *J. Quant. Spectrosc. Radiat. Transfer,* vol. 7, pp. 261-272, 1967.